## Dynamics of the Two-Site Hubbard Model

A. T. Costa Jr.\*and M. T. Thomaz<sup>†</sup>
Instituto de Física - Universidade Federal Fluminense
Av. Gal. Milton Tavares de Souza s/n°. - Gragoatá
Niterói, Rio de Janeiro 24210-340, Brazil

August 15, 2018

#### Abstract

The dynamical evolution of a two-site Hubbard model is derived in the presence of an uniform external magnetic field for a general initial state. The time evolution of the half-filled (two-particle) case has a complex behaviour. Under certain initial conditions, the average number of fermions in one-particle state, in the half-filled case, is not necessarily periodic, even though the magnetization remains periodic. The results obtained may be applied to study the magnetization and the transition dipole moment of the organic charge-transfer salts in the in-phase mode.

\*E-mail: antc@if.uff.br  $^{\dagger}$ E-mail: mtt@if.uff.br

### Dynamics of the Two-Site Hubbard Model

Even the simplest fermionic many-body model in Condensed Matter Physics, is too complicated to be treated exactly. This is the case of the well known Hubbard model [1]. Despite of its simplicity, it gives good qualitative descriptions of many important phenomena in Condensed Matter Physics. These results come from numerical simulations (of the Monte Carlo type, for example) or from a perturbative treatment of one of the terms in the hamiltonian [1]. Non-perturbative analytical treatment of the model turns out to be feasible if one further simplification is made: to consider a small number of space lattice wites. Although this simplification seems to impose serious limitations on the applicability of the model, it still can describe interesting phenomena occurring in real systems, e.g., the appearance of extra excitation lines in the infra-red spectra of organic charge-trasfer (CT) salts [4, 5, 6]. In the literature, this system is described by two-site Hubbard model[4, 5]. Usually, it has been studied energy-levels[5] and the optical properties of the CT salts in the presence of the external time dependent electric field [4], in the half-filled case. There are also experimental data of the energies of the peaks in the dimer spectrum for different temperature. In all previous work, the system is not studied in the presence of an external magnetic field.

The time dependence of the CT salts results is a consequence of an external electric field. However, it is missing the dynamics of the CT salts under general initial conditions of the vector state that describes the dimer.

In this work we present the exact time evolution of the two-site Hubbard model, with arbitrary band filling and coupling constant, in the presence of an uniform magnetic field. From an arbitrary many-body initial state we obtain the exact density operator of the system. The one-body properties of this identical particles system are obtained by calculating the one-particle reduced density matrix. These results give us a dynamical picture of the behaviour of the one-electron states of the system, and allow us to obtain the electron population in each one-particle state, the magnetization per site and the transition of the electric dipole moment of CT salts in the in-phase mode, in the presence of an external constant magnetic field.

The well-known Hubbard model [1] has the second-quantized hamil-

tonian

$$\mathbf{H} = \sum_{ij,\sigma} t_{ij} \mathbf{a}_{i,\sigma}^{\dagger} \mathbf{a}_{j,\sigma} + U \sum_{i,\sigma} \mathbf{n}_{i,\sigma} \mathbf{n}_{i,-\sigma} + \lambda_B \sum_{i} (\mathbf{n}_{i,\uparrow} - \mathbf{n}_{i,\downarrow}). \quad (1)$$

where  $\mathbf{a}_{j,\sigma}$  is the destruction operator of one electron with spin  $\sigma$  on site  $i,\ t_{ij}$  are the so-called hopping integrals, U is the effective intra-atomic Coulomb interaction,  $\lambda_B = -\frac{g\mu_B B}{2}$ , where g is the Landé factor,  $\mu_B$  is the Bohr magneton, B is the external magnetic field chosen in the  $\hat{z}$  direction, and  $\mathbf{n}_{i,\sigma} = \mathbf{a}_{i,\sigma}^{\dagger} \mathbf{a}_{i,\sigma}$ . The creation  $(\mathbf{a}_{i,\sigma}^{\dagger})$  and destruction  $(\mathbf{a}_{j,\sigma'})$  operators satisfy the anti-commutation relations:

$$\{\mathbf{a}_{i,\sigma}^{\dagger}, \mathbf{a}_{j,\sigma'}\} = \delta_{ij}\delta_{\sigma\sigma'},$$

$$\{\mathbf{a}_{i,\sigma}, \mathbf{a}_{j,\sigma'}\} = \{\mathbf{a}_{i,\sigma}^{\dagger}, \mathbf{a}_{j,\sigma'}^{\dagger}\} = 0.$$
(2)

We consider here the case where the hamiltonian (1) takes into account only nearest-neighbour hopping. We also have  $t_{11} = t_{22} = E_0$  and  $t_{12} = t_{21} = T$ . Under these conditions, a two-site Hubbard hamiltonian (1) describes, for example, the CT salts in the in-phase mode [4], but in absence of vibronic couping with the internal modes of the monomers. For the CT salt,  $E_0$  denotes the enrgy of the radical electron molecular orbital, T gives the hopping integrals of electrons between the molecules and U is the effective Coulomb interaction between the two electrons on the same molecule [5].

In order to study the most general state of the system for the two sites case, we choose a basis of eigenstates of the number operator  $\mathbf{n}_{i,\sigma}$ , whose components can be written as

$$|n_1 n_2; m_1, m_2\rangle = (\mathbf{a}_{1,\downarrow}^{\dagger})^{n_1} (\mathbf{a}_{1,\uparrow}^{\dagger})^{n_2} (\mathbf{a}_{2,\downarrow}^{\dagger})^{m_1} (\mathbf{a}_{2,\uparrow}^{\dagger})^{m_2} |0\rangle,$$
 (3)

where  $n_i, m_i = 0, 1$  and i = 1, 2.  $|0\rangle$  represents the vacuum state of the model.

The action of  $\mathbf{H}$  over each of the basis states can be obtained by straightforward calculation, using the anticommutation relations eq. (2).

The most general initial condition for the system described by a state vector is

$$|\Psi(0)\rangle = \sum_{n_1, n_2, m_1, m_2 = 0}^{1} f_{n_1, n_2, m_1, m_2}(0) |n_1 n_2; m_1 m_2\rangle,$$
 (4)

where  $|n_1n_2; m_1m_2\rangle$  are given by eq.(3) and the values of the constants  $f_{n_1,n_2,m_1,m_2}(0)$  are determined by the initial conditions. Due to the fact that the eigenstates of the number operator, eq. (3), form a complete basis, at any time we have,

$$|\Psi(t)\rangle = \sum_{n_1, n_2, m_1, m_2 = 0}^{1} f_{n_1, n_2, m_1, m_2}(t) |n_1 n_2; m_1 m_2\rangle.$$
 (5)

Inserting  $|\Psi(t)\rangle$  in the Schrödinger equation gives a system of coupled first order differential equations for the coefficients  $f_{n_1,n_2,m_1,m_2}(t)$  that can be solved analytically. Actually, before solving the coupled equations for the coefficients, it is worth to notice that, since  $[\mathbf{H}, \mathbf{N}_{\sigma}] = 0$ , where  $\mathbf{N}_{\sigma} = \sum_{i} \mathbf{n}_{\sigma,i}$ , this system of coupled equations brakes up in smaller set of systems. The dynamics of states with different spin components are decoupled. We end up with five systems of first order differential equations. In appendix A, we give the explicitly time evolution of each eigenstate of the total number operator  $(\mathbf{N} = \sum_{i,\sigma} \mathbf{n}_{\sigma,i})$ . Not all vectors belonging to basis (3) are eigenstates of the hamiltonian (1), but since  $\mathbf{N}$  and  $\mathbf{N}_{\sigma}$  are constants of motion, the eigenstates of  $\mathbf{H}$  are labeled by their eigenvalues of  $\mathbf{N}$  and  $\mathbf{N}_{\sigma}$ .

With the time-dependence of the most general state of the system in hands, we can write the time-dependent density matrix of this many-body system,

$$\rho(t) = |\Psi(t)\rangle\langle\Psi(t)|. \tag{6}$$

If we are interested in the effective dynamics of the one-particle subsystem, the one-body density matrix [2, 3] must be determined. It is defined in terms of the full density matrix as

$$\Lambda_{i,\sigma;j,\sigma'}(t) = Tr\{\mathbf{a}_{i,\sigma'}^{\dagger}\mathbf{a}_{i,\sigma} \,\rho(t)\}. \tag{7}$$

For the sake of simplicity, instead of working with four indices in the definition of  $\Lambda(t)$  we redefine them as:

$$\mathbf{a}_{1,\downarrow} \equiv \mathbf{a}_1, \quad \mathbf{a}_{2,\downarrow} \equiv \mathbf{a}_2, \quad \mathbf{a}_{1,\uparrow} \equiv \mathbf{a}_3, \quad \mathbf{a}_{2,\uparrow} \equiv \mathbf{a}_4,$$
 (8)

and in an analogous way the creation operators.

Using the new definition for the indices, and, the fact that  $\rho(t)$  is a pure density matrix, the trace in eq.(7) reduces to

$$\Lambda_{ij}(t) = \langle \Psi(t) | \mathbf{a}_i^{\dagger} \mathbf{a}_i | \Psi(t) \rangle \qquad i, j = 1, \dots, 4.$$
 (9)

It is clear from the definition (7) that the diagonal elements of  $\Lambda(t)$  give the average population of the one-particle state i for the identical particle system described by  $|\Psi(t)\rangle$ . From these elements, other important quantities may be determined, such as magnetization per site<sup>1</sup> and electric dipole moment<sup>2</sup>. It is interesting to notice that, although the whole system is in a pure state, the effective one-body subsystem, depending on the initial values of  $f_{n_1,n_2,m_1,m_2}(0)$ , is in a statistical mixture of states. This may be easily verified by direct calculation of  $\Lambda^2(t)$  and subsequent comparison with  $\Lambda(t)$  itself. In general, we get  $\Lambda^2(t) \neq \Lambda(t)$ , in a clear indication of the statiscal mixture character of the one-particle subsystem state.

Although we have an analitical expression for the most general state of the system  $|\Psi(t)\rangle$ , it is very cumbersome and not worth showing here (look in Appendix A for the time dependence of the coefficients  $f_{m_1m_2n_1n_2}(t)$  eq. (5)). Instead, we choose a set of numerical values for the constants of the model and some initial states  $|\Psi(0)\rangle$ , and present the results for some one-particle quantities.

The zero- and four-particle sectors of the Fock space are very uninteresting. They have only one vector each, which evolves in time only by a phase. If the initial state  $|\Psi(0)\rangle$  lies entirely in one of these sectors, all the one-particle observables are constant in time.

The one- and three-particle sectors have both four vectors, and are divided into two sets of two coupled vectors each. If  $|\Psi(0)\rangle$  lies within one of these sectors, the one-particle observables are time-dependent

$$\mathbf{m}_{i}^{z} = -g\mu_{B}(\mathbf{n}_{i,\uparrow} - \mathbf{n}_{i,\downarrow}),\tag{10}$$

where g is the Landé factor and  $\mu_B$  is the Bohr magneton.

<sup>2</sup> The electron electric dipole moment of the dimer[8]:

$$\vec{\mathbf{p}} = \frac{e\vec{a}}{2}(\mathbf{n}_1 - \mathbf{n}_2),\tag{11}$$

where  $\mathbf{n}_i = \sum_{\sigma=\uparrow,\downarrow} \mathbf{n}_{i,\sigma}$ .

<sup>&</sup>lt;sup>1</sup> The z component of the magnatization of site i is [8]

in general, being periodic functions of time with the frequency  $\frac{T}{\hbar}$ . Since the dynamics does not couple different Fock sub-spaces, the diagonal elements of the  $\Lambda$  matrix in these two Fock-subspaces are:

$$\Lambda_{11}^{(1)} = |f(1,0;0,0;0)|^2 \cos^2(\frac{Tt}{\hbar}) + |f(0,0;1,0;0)|^2 \sin^2(\frac{Tt}{\hbar}),$$
(12)

$$\Lambda_{33}^{(1)} = |f(1,0;1,1;0)|^2 + |f(1,1;1,0;0)|^2 + 
+ |f(1,1;0,1;0)|^2 \cos^2(\frac{Tt}{\hbar}) + |f(0,1;1,1;0)|^2 \sin^2(\frac{Tt}{\hbar})$$
(13)

and

$$\Lambda_{11}^{(3)} = |f(0,1;0,0;0)|^{2} \cos^{2}(\frac{Tt}{\hbar}) + |f(0,0;0,1;0)|^{2} \sin^{2}(\frac{Tt}{\hbar}),$$

$$\Lambda_{33}^{(3)} = |f(0,1;1,1;0)|^{2} + |f(1,1;0,1;0)|^{2} +$$

$$+ |f(1,1;1,0;0)|^{2} \cos^{2}(\frac{Tt}{\hbar}) + |f(1,0;1,1;0)|^{2} \sin^{2}(\frac{Tt}{\hbar}),$$
(15)

where  $\Lambda_{ii}^{(1)}$  are diagonal elements of the one-particle reduced density matrix in the Fock sub-space N=1 and  $\Lambda_{ii}^{(3)}$  the diagonal elements for N=3. In the solid-state language, these two sectors correspond to the quarter and three-quarter band filling of the model respectively. Due to the particle-hole symmetry of the model, these two sectors have very similar characteristics. Note that when the state has three fermionic particles, there is interaction among them. However, we see from eqs. (14) and (15) that the dynamics of theses states is only dictated by the hopping integral T, as is compatible with particle-hole symmetry.

The operator  $\mathbf{N}_{\sigma}$  is a constant of motion. To describe the dynamics of the one-particle sub-system it is enough to discuss, for fixed  $\sigma$ , the population in one of the space sites. We have chosen to fix in eqs. (12)-(13) and eqs.(14)-(15) on site i=1.

The two-particle sector has the richest structure, for it has six state vectors, where four of them are coupled. If we choose  $|\Psi(0)\rangle$  to lie in this sector, the one-particle observables are in general quasiperiodic functions of time. The time dependence of the population of each one-particle observable has two frequencies:  $w_1 = \frac{U}{2\hbar}$  and  $w_2 = \frac{\sqrt{U^2 + 16T^2}}{2\hbar}$ . In general,  $\frac{w_1}{w_2} \neq \frac{p}{q}$ , where p and q are integers, which implies that the dynamics of the population of the one-particle subsystem is not periodic in general. For some special initial states, only a few of the one-particle observables turn out to be periodic. This happens because of subtle cancellations occurring in the calculations of those observables, as will be shown later on. This sector correspond to the half-filled Hubbard model, widely studied in solid state physics. In particular, this is the band-filling used to describe the charge-trasfer organic salts [4, 5].

In order to ilustrate the qualitative discussion given above, we present some graphs for one-particle observables obtained from the analytical expressions. We need to point out that the external constant magnetic field only appears in the phases of the time evolution of states (3) of the Fock sub-spaces  $N=1,\,N=3$  and for states of N=2 when both fermions have the same spin component. But, in the one-particle reduced density matrix, it gives no contribution. Let us consider the graphs when the model constants are chosen as:

$$T = 1$$
 $U = 0.5$ ,
 $\lambda_B = 0$ . (16)

We have taken  $\hbar=1$ . In doing this,  $T/\hbar$  turns out to be an energy scale for the system. We first chose U comparable to the hopping integral T to see how the two terms in the Hamiltonian combine when none of them is dominating. This competition reveals itself in the time-dependence of the one-particle observables by the absence of a characteristic frequency in their oscillations. In figure 1 we show the average spin up occupation  $n_{1\uparrow} = \Lambda_{1\uparrow,1\uparrow} \equiv \Lambda_{33}(t)$ , and the average electric dipole moment of the dimmer  $d(t) = \Lambda_{2\uparrow,2\uparrow}(t) + \Lambda_{2\downarrow,2\downarrow}(t) - (\Lambda_{1\uparrow,1\uparrow}(t) + \Lambda_{1\downarrow,1\downarrow}(t)) \equiv \Lambda_{22}(t) + \Lambda_{44}(t) - (\Lambda_{33}(t) + \Lambda_{11}(t))$  for the initial state  $|\Psi_1(0)\rangle = |11\rangle|00\rangle$ . It is easy to identify both functions as non-periodic by simply looking at the figures. The average magne-

tization per site of this state is zero, since its initial value is zero and it is a constant of motion.

If we now choose a new initial state  $|\Psi_2(0)\rangle = \frac{1}{\sqrt{3}}(|10\rangle|01\rangle - |01\rangle|10\rangle + |11\rangle|00\rangle$ , we obtain two non-periodic observables, namely  $n_{1\uparrow}(t)$  and  $d_1(t)$ , but the average magnetization of site 1,  $m_1(t) = \Lambda_{1\uparrow,1\uparrow}(t) - \Lambda_{1\downarrow,1\downarrow}(t)$ , turns out to be periodic (see Figure 2). This occurs because of a cancellation of the contributions from  $|10\rangle|01\rangle$  and  $|01\rangle|10\rangle$  to the average magnetization per site, due to the fact that both states enter the combination with coefficients of same modulus but opposite sign.

In order to ilustrate how the relation between the hopping integral T and the Coulomb interaction U may influence the observables of the system, we choose a new set of model constants, and repeat the calculations already performed. In the literature[6] it is stated that for the CT salts U=5.45T, therefore, we choose the new set of constants as:

$$T = 1$$
  
 $U = 5.45$ ,  
 $\lambda_B = 0$ . (17)

Now the Coulomb interaction U is four times greater than the hopping integral T. In figure 3 we observe that this noticeable difference between them causes the appearance of a modulation of frequencies. The higher frequency oscilations due to the Coulomb integral are superimposed to the hopping integral oscilations.

In summary, we studied the exact dynamics of two-site Hubbard model when the identical particles system is described by a vector state. We considered the case where  $t_{12} = t_{21} = T$ , that has been used as a model to explain the CT salts in the in-phase mode [4], without the interaction of the radical electrons with the internal vibronic modes of the molecule.

The particle–hole simmetry of the Hubbard model is well realized by the time evolution of  $\Lambda^{(3)}_{ii}$ , i=1,2. Even though for the three-particle Fock sub-space the Coulomb interaction (1) still works, the dynamics of the population of one-particle states is governed by the hopping integral T, as happens for the Fock sub-space N=1.

In the half-filled case, depending on the initial conditions, we can get non-periodic behaviour for some one-particle properties, while the magnetization per site remains periodic.

Finally, we have shown as the one-particle observables as magnetization and site occupation oscillate in time. It is well known that, when these quantities are measured in real systems as magnetic transition metals for example, the measurements furnish constant fractional values. From the theory of intinerant magnetism we have that the measured fractional charge and magnetization of such metals is a consequence of a time average performed by the measuring apparatus. We obtain fractional values by taking the time average of the time-dependent observables we have calculated. This time average is defined as

$$\langle w(t) \rangle = \lim_{T \to \infty} \frac{1}{T} \int_0^T w(t)dt$$
. (18)

For the half-filled case, we get from eq.(18) and what was discussed previously, that the average value for the magnetization per site is a fractional constant, but the eletric dipole transition is not, since it is not a periodic function in time. We get a time dependent electric polarizability in the absence of an external electric field. It is an open question if this effect can actually be measured.

## Acknowledgements

A.T.C. Jr. thanks CNPq for financial support and M.T.T. thanks CNPQ and FINEP for partial financial support. We also thank J.J. Rodriguez Nuñes for bringing reference [5] to our attention.

# Appendix A: Time Evolution of the Eigenstates of $n_{i,\sigma}$ Operator

In this apendix we present the explicit time dependence of the most general state of the two-site Hubbard model. It is obtained by inserting

$$|\Psi(t)\rangle = \sum_{m_1, m_2, n_1, n_2=0}^{1} f_{m_1 m_2 n_1 n_2}(t) |m_1 m_2\rangle |n_1 n_2\rangle$$
 (19)

in the Schrödinger equation, and then projecting out this equation over each one of the basis states (3). This will, in principle, give a set of sixteen coupled first order differential equations for the  $f_{m_1m_2n_1n_2}(t)$ . Due to some simetries of the Hamiltonian, these sixteen equations decouple, forming a set of five independent systems with variable number of equations. From the hamiltonian (1), we have the folling constants of motion:

$$[\mathbf{H}, \mathbf{N}_{\sigma}] = 0,$$
  
$$[\mathbf{H}, \mathbf{N}] = 0.$$
 (20)

Eq.(20) leads to total charge and spin conservation of the hamiltonian, which defines five independent sectors of the Hilbert space, labeled by the total charge of the states. These sectors may be further divided in subsectors of states with the same total spin (or magnetization). Therefore we may determine the dynamics of each subsector independently. The explicit time dependence of each coefficient  $f_{m_1m_2n_1n_2}(t)$  is given below.

#### Fock sub-space N=0:

$$f_{0000}(t) = f_{0000}(0) (21)$$

#### Fock sub-space N=1:

Subsector  $\sigma = \downarrow$ :

$$f_{1000}(t) = \left[f_{1000}(0)cos(\frac{t_{12}t_{21}}{\hbar}t) - i\frac{|\tau|}{\tau^*}f_{0010}(0)sin(\frac{t_{12}t_{21}}{\hbar}t)\right]e^{-i\frac{(\epsilon-\lambda_B)}{\hbar}t}$$
(22)

$$f_{0010}(t) = \left[f_{0010}(0)\cos(\frac{t_{12}t_{21}}{\hbar}t) - i\frac{|\tau|}{\tau}f_{1000}(0)\sin(\frac{t_{12}t_{21}}{\hbar}t)\right]e^{-i\frac{(\epsilon-\lambda_B)}{\hbar}t}$$
(23)

Subsector  $\sigma = \uparrow$ :

$$f_{0100}(t) = \left[f_{0100}(0)cos(\frac{t_{12}t_{21}}{\hbar}t) - i\frac{|\tau|}{\tau^*}f_{0001}(0)sin(\frac{t_{12}t_{21}}{\hbar}t)\right]e^{-i\frac{(\epsilon-\lambda_B)}{\hbar}t}$$
(24)

$$f_{0001}(t) = \left[f_{0001}(0)cos(\frac{t_{12}t_{21}}{\hbar}t) - i\frac{|\tau|}{\tau}f_{0100}(0)sin(\frac{t_{12}t_{21}}{\hbar}t)\right]e^{-i\frac{(\epsilon-\lambda_B)}{\hbar}t}$$
(25)

#### Fock sub-space N=2:

Subsector  $\sigma = 0$ :

$$f_{1100}(t) = i \frac{|\tau|^2}{\tau^* \beta} sin(\frac{\beta}{\hbar} t) (f_{0110}(0) - f_{1001}(0)) + \frac{1}{2\beta \tau^*} [\beta cos(\frac{\beta}{\hbar} t) - iU sin(\frac{\beta}{\hbar} t)] \times (\tau f_{0011}(0) + \tau^* f_{1100}(0)) e^{-i\frac{(2\epsilon + U)}{\hbar} t} - \frac{1}{2\tau^*} e^{-2i\frac{(\epsilon + U)}{\hbar} t} (\tau f_{0011}(0) - \tau^* f_{1100}(0))$$
(26)

$$f_{0011}(t) = i \frac{|\tau|^2}{\tau \beta} sin(\frac{\beta}{\hbar}t) (f_{0110}(0) - f_{1001}(0)) + \frac{1}{2\beta \tau} [\beta cos(\frac{\beta}{\hbar}t) - iUsin(\frac{\beta}{\hbar}t)] \times \\ \times (\tau f_{0011}(0) + \tau^* f_{1100}(0)) e^{-i\frac{(2\epsilon + U)}{\hbar}t} + \frac{1}{2\tau} e^{-2i\frac{(\epsilon + U)}{\hbar}t} (\tau f_{0011}(0) - \tau^* f_{1100}(0))$$

$$(27)$$

$$f_{1001}(t) = \frac{1}{2} (f_{0110}(0) + f_{1001}(0)) e^{-2i\frac{\epsilon}{\hbar}t} - \{\frac{i}{\beta} [\tau f_{0011}(0) + \tau^* f_{1100}(0) + \frac{U}{2} (f_{0110}(0) - f_{1001}(0)] sin(\frac{\beta}{\hbar}t) - \frac{1}{2} (f_{0110}(0) - f_{1001}(0)) cos(\frac{\beta}{\hbar}t) \} e^{-i\frac{(2\epsilon + U)}{\hbar}t}$$

$$(28)$$

$$f_{0110}(t) = \frac{1}{2} (f_{0110}(0) + f_{1001}(0)) e^{-2i\frac{\epsilon}{\hbar}t} + \{\frac{i}{\beta} [\tau f_{0011}(0) + \tau^* f_{1100}(0) + \frac{U}{2} (f_{0110}(0) - f_{1001}(0)] sin(\frac{\beta}{\hbar}t) - \frac{1}{2} (f_{0110}(0) - f_{1001}(0)) cos(\frac{\beta}{\hbar}t) \} e^{-i\frac{(2\epsilon + U)}{\hbar}t}$$
(29)

Subsector  $\sigma = -1$ :

$$f_{1010}(t) = e^{-2i\frac{(\epsilon - \lambda_B)}{\hbar}t} f_{1010}(0)$$
(30)

Subsector  $\sigma = 1$ :

$$f_{0101}(t) = e^{-2i\frac{(\epsilon + \lambda_B)}{\hbar}t} f_{0101}(0)$$
(31)

#### Fock sub-space N=3:

Subsector  $\sigma = \downarrow$ :

$$f_{1110}(t) = \left[i\frac{|\tau|}{\tau^*}f_{1011}(0)sin(\frac{|\tau|}{\hbar}t) + f_{1110}(0)cos(\frac{|\tau|}{\hbar}t)\right]e^{-i\frac{(3\epsilon+2U-\lambda_B)}{\hbar}t}$$
(32)

$$f_{1011}(t) = \left[i\frac{|\tau|}{\tau}f_{1110}(0)sin(\frac{|\tau|}{\hbar}t) + f_{1011}(0)cos(\frac{|\tau|}{\hbar}t)\right]e^{-i\frac{(3\epsilon+2U-\lambda_B)}{\hbar}t}$$
(33)

Subsector  $\sigma = \uparrow$ :

$$f_{1101}(t) = \left[i\frac{|\tau|}{\tau^*}f_{0111}(0)sin(\frac{|\tau|}{\hbar}t) + f_{1101}(0)cos(\frac{|\tau|}{\hbar}t)\right]e^{-i\frac{(3\epsilon + 2U + \lambda_B)}{\hbar}t}$$
(34)

$$f_{0111}(t) = \left[i\frac{|\tau|}{\tau}f_{1101}(0)sin(\frac{|\tau|}{\hbar}t) + f_{0111}(0)cos(\frac{|\tau|}{\hbar}t)\right]e^{-i\frac{(3\epsilon+2U+\lambda_B)}{\hbar}t}$$
(35)

#### Fock sub-space N=4:

$$f_{1111}(t) = e^{-4i\frac{(\epsilon+U)}{\hbar}t} f_{1111}(0)$$
(36)

Here,  $f_{m_1m_2n_1n_2}(0)$  is the coefficient of the  $|mm_2\rangle|n_1n_2\rangle$  state at t=0,  $\tau=t_{12}=t_{21}^*$  and  $\beta=\sqrt{U^2+4|\tau|^2}$ .

## References

- [1] J. Hubbard, Proc. Roy. Soc. A277 (1963) 237; A281 (1964) 401.
- [2] R.P. Feynman, Statistical Mechanics: A Set of Lectures (Addison-Wesley, 1980), Chap. 2.
- [3] P. Ring and P. Schuck, *The Nuclear Many-Body Problem* (Springer-Verlag, New York, 1980) pp 245-248 and 251-252.
- [4] M.J. Rice, Solid State Comm. **31** (1979) 93.
- [5] M.E. Kozlov, V.A. Ivanov and K. Yakushi, *J. Phys.: Condens. Matter* 8 (1996) 1011.
- [6] J.B. Torrence, B.A. Scott, B. Welber, F.B. Kaufman and E. Seiden, *Phys. Rev.* B19 (1979) 730.
- [7] M.J. Rice, V.M. Yartsev and C.S. Jacobsen, *Phys. Rev.* B21 (1980) 3437.
- [8] C. Kittel, Introduction to Solid State Physics,  $7^{\rm th}$  edition ( John Willey & Sons, 1996).

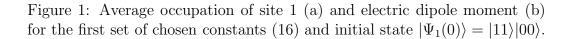


Figure 2: Average occupation (a) and magnetization (b) of site 1 and electric dipole moment (c) for the first set of chosen constants and initial state  $|\Psi_2(0)\rangle$ . Observe the non periodicity of (a) and (c), in contrast to (b), which is clearly periodic.

Figure 3: Average occupation of site 1(a) and electric dipole moment(b) for the second set of chosen constants (17) and initial state  $|\Psi_2(0)\rangle$ . Contrary to what was seen in figs. 1 and 2, these observables present two clearly distinct characteristic frequencies superimposed, due to the discrepancy between the hopping integral and the Coulomb interaction.

